# Energy Efficiency of Small Cell Backhaul Networks Based on Gauss-Markov Mobile Models

Xiaohu Ge<sup>1</sup>, Song Tu<sup>1</sup>, Tao Han<sup>1</sup>, Qiang Li<sup>1</sup>, Guoqiang Mao<sup>2</sup>,

<sup>1</sup>Department of Electronics and Information Engineering
Huazhong University of Science and Technology, Wuhan 430074, Hubei, P. R. China.
Email: {xhge, u201013039, hantao, qli\_patrick}@mail.hust.edu.cn

<sup>2</sup>School of Computing and Communication
The University of Technology Sydney, Australia and National ICT Australia (NICTA), Sydney
Email: g.mao@ieee.org

#### Abstract

To satisfy the recent growth of mobile data usage, small cells are recommended to deploy into conventional cellular networks. However, the massive backhaul traffic is a troublesome problem for small cell networks, especial in wireless backhaul transmission links. In this paper, backhaul traffic models are first presented considering the Gauss-Markov mobile models of mobile stations (MSs) in small cell networks. Furthermore, an energy efficiency model of small cell backhaul networks with Gauss-Markov mobile models has been proposed. Numerical results indicate that the energy efficiency of small cell backhaul networks can be optimized by trade-off the number and radius of small cells in cellular networks.

#### **Index Terms**

Energy efficiency, backhaul traffic, small cell networks, Gauss-Markov mobile model

Correspondence author: Dr. Tao Han, Email: hantao@mail.hust.edu.cn

The authors would like to acknowledge the support from the International Science and Technology Cooperation Program of China (Grant No. 2014DFA11640 and 2012DFG12250), the National Natural Science Foundation of China (NSFC) (Grant No. 61271224, 61471180 and 61301128), NFSC Major International Joint Research Project (Grant No. 61210002), the Hubei Provincial Science and Technology Department (Grant No. 2013BHE005), the Fundamental Research Funds for the Central Universities (Grant No. 2011QN020, 2013QN136, 2014QN155 and 2013ZZGH009), Special Research Fund for the Doctoral Program of Higher Education (SRFDP) (Grant No. 20130142120044), and EU FP7-PEOPLE-IRSES (Contract/Grant No. 247083, 318992 and 610524).

#### I. INTRODUCTION

To improve the capacity of wireless communication systems, one of potential solutions is to reduce the coverage of cellular scenarios and close users to base stations (BSs) [1]. Therefore, small cell technologies, including femtocell, picocell and microcell technologies are emerging into cellular networks [2]. With millimeter wave communications adopting in small cel BSs, the small cell is able to load with massive traffic in future fifth generation (5G) mobile communication systems. However, it is a great challenge to realize wireless massive backhaul traffic in small cell networks by an energy efficiency way [3].

With small cell technologies adopted into wireless communication systems, small cell networks were studied in recently literatures [4]-[8]. The overall outage probability and the symbol error probability were analyzed for small cell networks where BS locations are generated according to a Poisson distribution and linear multiuser precoding is employed for wireless communications [4]. Based on the network multiple-input-multiple-output (MIMO) technology of small cell networks, a coalition formation game model was proposed to cluster small cell BSs and performed the cluster-wise joint beamforming into wireless cooperation transmissions [5]. Taking into account the retrial phenomenon, the finite number of users served in a cell and the random breakdowns of BS channels, a new computational approach was presented to evaluate the reliability of small cell networks using the Generalized Stochastic Petri Nets (GSPNs) theory [6]. In the small cell deployment, the large number of small cells conduces to the increase of signaling load due to frequently handoff and the mobility robustness to be degraded due to increased handoff failures and radio link failures. When the large number of small cells are deployed in the LTE-Advance mobile communication systems, the impact of small cell deployment on the mobility performance of LTE-Advance mobile communication systems was evaluated in [7] by system level simulations. The analytical results of the user signal-to-interference-and-noise ratio (SINR) quality in random small cell networks under log-normal interferers were presented and the spatial outage and throughput were compared between the random topology and the regular topology in small cell networks [8].

Currently improving energy efficiency of wireless networks is widely concerned by industries and academics [9]–[15]. A brief survey of methods to improve the power efficiency of cellular networks was presented in [10]. Moreover, some research issues and challenges were explored for future green cellular networks. Contrary to conventional energy efficiency of wireless networks, the embodied energy was accounted for the energy efficiency evaluation of wireless networks in whole production lifetime [11]. Assuming that BSs and users are modeled by two independent spatial Poisson point processes, the energy efficiency of small cell networks were analyzed for different densities of BSs in small cellular scenarios [12]. Another type of small cell network, i.e., femtocell networks was investigated for evaluating the energy efficiency of two-tier cellular networks with partially open channels [13]. Based on the random spatial network model where BSs and users are modeled by two independent spatial Poisson point processes, an analytical framework for downlink performance analysis of small cell networks was developed for throughput and energy efficiency evaluation [14]. The energy efficiency of heterogeneous wireless networks was investigated by introducing the area energy efficiency concept [15]. Simulation results demonstrate that both cell

energy efficiency and area energy efficiency can be improved by deploying low power pico BSs combined with reduction of macro transmission power.

Some studies explored the backhaul traffic in small cell networks [16]–[18]. Based on the IMT-A standard, the proportion of different types of backhaul traffic in small cell networks was specified in [16]. Furthermore, the backhaul traffic requirement was evaluated for the heterogeneous networks where small cells are embedded into macrocells and the inter-site cooperation is featured to improve the network performance [17]. Moreover, the bandwidth requirement for sharing information among cooperative BSs was investigated for network MIMO as a function of the cooperative cluster size and channel characteristics [18]. However, in all the aforementioned small cell network studies, only simple scenarios, such as user terminals are assumed to be stationary or a simple linear mobility, were considered for backhaul traffic modeling. Besides, the energy efficiency of small cell backhaul networks with Gauss-Markov mobile model of mobile stations (MSs) is surprising rare in the open literature.

Motivated by the above gaps, in this paper we derive the energy efficiency model of small cell backhaul networks with MSs Gauss-Markov mobile models. The contributions and novelties of this paper are summarized as follows.

- 1) We propose the backhaul traffic models for small cell networks based on MSs Gauss-Markov mobile models.
- From the proposed backhaul traffic models, we derive an energy efficiency model of small cell backhaul networks with MSs Gauss-Markov mobile models.
- 3) We simulate the energy efficiency of small cell backhaul networks in great details and present some interesting observations.

The remainder of this paper is outlined as follows. Section II describes the system model of small cell networks and the handoff rate of small cells considering the Gauss-Markov mobile model of MSs. In Section III, the backhaul traffic models are proposed for small cell networks with Gauss-Markov mobile models. The energy efficiency of small cell backhaul networks is derived for performance analysis in Section IV. Numerical results imply that the number and the radius of small cells have great impact on the energy efficiency of small cell backhaul networks. Finally, conclusions are drawn in Section V.

#### II. SYSTEM MODEL

## A. Gauss-Markov mobile models

Gauss-Markov mobile models are widely used for describing MS mobility in different dimensionalities. Considering that small cells and MSs are deployed in a two-dimensional (2-D) plane, the 2-D Gauss-Markov mobile model is introduced for modeling of MSs' mobility in small cell networks. Without loss of generality, the location vector and the velocity vector of a MS are denoted as  $\overline{s_n} = [s_n^x, s_n^y]^T$  and  $\overline{v_n} = [v_n^x, v_n^y]^T$ , where  $n \in [0, \infty)$  is a non-negative integer,  $x \in (-\infty, +\infty)$  and  $y \in (-\infty, +\infty)$  are dimensions in a Euclid coordinate. Moreover, the memory level vector of mobile velocity is represented by  $\overline{\alpha} = [\alpha^x, \alpha^y]^T$ , the mean vector and standard deviation vector of mobile velocity are represented by  $\overline{\mu} = [\mu^x, \mu^y]^T$  and  $\overline{\sigma} = [\sigma^x, \sigma^y]^T$ , respectively. Then, the 2-D velocity process of MS is expressed as follows

$$\overline{v_n} = \overline{\alpha} \odot \overline{v_{n-1}} + (E - \overline{\alpha}) \odot \overline{\mu} + \overline{\sigma} \odot \sqrt{E - \overline{\alpha} \odot \overline{\alpha}} \odot \overline{w_{n-1}}, \tag{1}$$

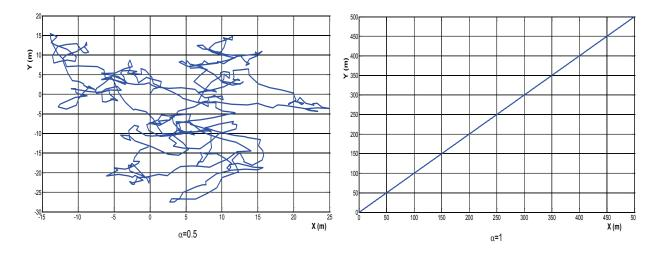


Fig. 1. Gauss-Markov mobile traces with different memory levels  $\alpha$ .

where  $\odot$  is the element-by-element multiplication, E is the  $2 \times 1$  identity matrix, the random elements of  $\overline{w_n}$  vector are governed by a Gauss distribution with zero mean and standard variance,  $\overline{w_n}$  and  $\overline{v_n}$  are independent each other. Moreover, random vectors in (1) are assumed to be uncorrelated in both dimensions. To simplify derivation, the velocity vector is assumed to have the same memory level  $\alpha$ , the same mean  $\mu$  and the same standard deviation  $\sigma$  in both dimensions. Furthermore, the velocity process of MS in small cell networks is expressed as

$$\overline{v_n} = \alpha \overline{v_{n-1}} + (1 - \alpha) \overline{\mu} + \sigma \sqrt{1 - \alpha^2} \overline{w_{n-1}}.$$
 (2)

The Gauss-Markov mobile model is not only used for describing the MS mobility in last slots but also used for predicting the MS mobility at the current slot. Based on the recurrence expression in (2), the MS mobility at current slot can be derived when the velocity and location of MS in last slots are known. For example, when the initial velocity of MS is denoted as  $\overline{v_0}$ , the MS velocity at the nth slot is derived as

$$\overline{v_n} = \alpha^n \overline{v_0} + (1 - \alpha^n) \overline{\mu} + \sigma \sqrt{1 - \alpha^2} \sum_{i=0}^{n-1} \alpha^{n-i-1} \overline{w_i}.$$
(3)

Similarly, the MS location at the nth slot in small cell networks can be derived by

$$\overline{s_n} = \overline{s_{n-1}} + \overline{v_{n-1}}. (4)$$

When the initial location of MS is configured as  $\overline{s_0} = 0$ , the MS location at the nth slot is derived as

$$\overline{s_n} = \sum_{i=0}^{n-1} \overline{v_i} = \frac{1 - \alpha^n}{1 - \alpha} \overline{v_0} + \left(1 - \frac{1 - \alpha^n}{1 - \alpha}\right) \mu + \sigma \sqrt{1 - \alpha^2} \sum_{i=0}^{n-1} \sum_{j=0}^{i-1} \alpha^{i - i - 1} \overline{w_j}.$$
 (5)

Moreover, the location random vector of MS follows a Gaussian process considering that the velocity random vector of MS is governed by Gaussian distributions.

The memory level  $\alpha$ ,  $0 < \alpha \le 1$ , of MS is used for representing the memory trace in a random walk process. When  $0 < \alpha \le 1$ , the trace of user mobility is expanded in a 2-D plane, which is suitable for describing the MS

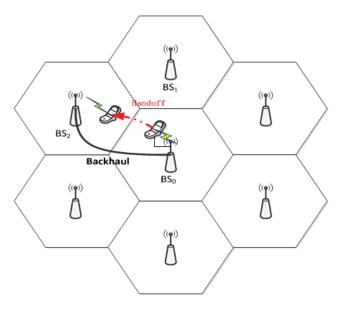


Fig. 2. MS handoff in small cell networks.

random mobility in a small cell network. Without loss of generality, the trace of random MS is illustrated in Fig. 1(a) when the memory level of MS is configured as  $\alpha = 0.5$ . When  $\alpha = 1$ , the trace of user mobility is expanded in a one dimension space and illustrated in Fig. 1(b), which is suitable for describing the MS mobility in trafficway scenarios.

#### B. Handoff rate in small cell networks

In LTE-A standards, the wireless backhaul link between the small cell and the macrocell is defined as the S1 link, which is used for exchanging traffic between small cell BSs and the core network [19]. The wireless backhaul link among small cells is defined as the X2 link, which is used for enabling the mutual information in small cells. Fig. 2 illustrates the MS handoff process in small cell networks. One small cell has one BS located at the center. To simplify the derivation, the coverage of every small cell is assumed as a regular hexagon and a small cell is adjoined by other six small cells. When a MS moves from the  $BS_0$ 's coverage to the  $BS_2$ 's coverage, X2 links forward the mutual information between the  $BS_0$  and  $BS_2$  to guarantee the success handoff. Moreover, the MS's data traffic is transmitted by S1 links.

To keep a balance in a stationary system, the outgoing traffic rate of MSs is assumed to be equal to the entering traffic rate of MSs in a small cell. The velocity of MS is decomposed in x and y dimensions as  $v_{nx}$  and  $v_{ny}$ , which are expressed by

$$v_{nx} = \alpha^n v_{0x} + (1 - \alpha^n) \mu + \sigma \sqrt{1 - \alpha^2} \sum_{i=0}^{n-1} \alpha^{n-i-1} w_{ix},$$
 (6a)

$$v_{ny} = \alpha^n v_{0y} + (1 - \alpha^n) \mu + \sigma \sqrt{1 - \alpha^2} \sum_{i=0}^{n-1} \alpha^{n-i-1} w_{iy}.$$
 (6b)

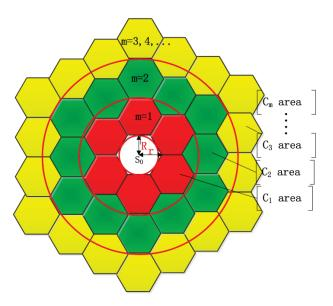


Fig. 3. Illustration of handoff number in small cell networks.

Without loss of generality, the initial velocity of MS in x and y dimensions is assumed as  $v_{0x} = 0$  and  $v_{0y} = 0$ , respectively. The mean of MS's velocity is assumed as  $\mu = 0$ . Furthermore, the speed of MS in x dimension is derived as

$$v_{nx} = \sqrt{1 - \alpha^2} \cdot \sum_{i=0}^{n-1} \alpha^{n-i-1} w_{ix}, \tag{7}$$

where  $w_{ix}$  is the random variable projected by the  $\overline{w_n}$  vector at x dimension, which is governed by a Gaussian distribution  $w_{ix} \sim N(0,1)$ . Therefore, the speed of MS in x and y dimensions also follow Gaussian distributions, i.e.,  $v_{nx} \sim N(0,\sigma_0^2)$  and  $v_{ny} \sim N(0,\sigma_0^2)$ , respectively. Furthermore, the speed of MS is expressed as

$$V = |v_n| = \sqrt{v_{nx}^2 + v_{ny}^2},\tag{8}$$

where V follows a Rice distribution. Then, the Cumulative Distribution Function (CDF) of the MS speed V is expressed by

$$F(v) = P(V < v) = 1 - exp(-\frac{v^2}{2\sigma_0^2}), v \ge 0,$$
(9)

where P is the probability operation. Assuming that the MS speed keeps the constant in one slot. The MS mobile distance in one slot is  $L_n = ||S_n - S_{n-1}|| = |v_n|$ . Then, the CDF of the MS mobile distance  $L_n$  is derived by

$$F(l) = P(L_n < l) = 1 - \exp(-\frac{l^2}{2\sigma_0^2}), l \ge 0.$$
(10)

Fig. 3 illustrates the MS mobility and handoff number in one slot of small cell networks. Without loss generality, the MS initial location  $S_0$  is assumed to be located at the origin point. In the next slot, the probability density function (PDF) of MS location  $S_1$  located at a circular ring with the radius  $\rho$  is derived as

$$f_{S1}(\rho) = \lim_{\Delta \rho \to 0} \frac{P(L \leqslant \rho + \Delta \rho) - P(L \leqslant \rho)}{2\pi \int_{\rho}^{\rho + \Delta \rho} x dx}$$

$$= \lim_{\Delta \rho \to 0} \frac{exp(-\frac{\rho^2}{2\sigma_0^2}) - exp[-\frac{(\rho + \Delta \rho)^2}{2\sigma_0^2}]}{2\pi \rho \Delta \rho}$$

$$= \frac{1}{2\pi \sigma_0^2} \exp(-\frac{\rho^2}{2\sigma_0^2}),$$
(11)

where  $\triangle \rho$  is the width of circular ring.

The expectation of MS handoff number N in one slot of small cell networks is expressed as

$$\mathbb{E}\{N\} = \sum_{m=1}^{\infty} m \int_{C_m} P(dA(\rho)), \tag{12}$$

Where  $\mathbb{E}$  is the expectation operation,  $P(dA(\rho))$  is the probability distribution of the random point with the PDF  $f_{S1}(\rho)$  given in (11),  $C_m$  is the area of small cells in the mth circular ring marked in Fig. 3. Moreover, the area  $C_m$  of small cells in the mth circular ring is approximated by

$$C_m \approx 2\pi \int_{(2m-1)R}^{(2m+1)R} \rho d\rho, \tag{13}$$

where  $R = \frac{\sqrt{3}}{2}r$  and r is the radius of small cell. Substitute (13) into (12), the expectation of MS handoff number N in one slot is derived by

$$\mathbb{E}\{N\} = \sum_{m=1}^{\infty} 2\pi m \int_{(2m-1)R}^{(2m+1)R} f_{S1}(\rho) \rho d\rho$$

$$= \sum_{m=0}^{\infty} \exp(-\frac{3\sqrt{3}}{4\pi\sigma_0^2} (2m+1)^2 r^2)$$

$$= \frac{2\sqrt{6}\sigma_0}{3\sqrt{\pi}r}.$$
(14)

A MS handoff rate H in small cell networks is defined as the expectation of MS handoff number in a slot. Based on (7), the speeds of MS in x and y dimensions also follow Gaussian distributions, i.e.,  $v_{nx} \sim N(0, \sigma_0^2)$  and  $v_{ny} \sim N(0, \sigma_0^2)$ , where  $\sigma_0 = (1 - \alpha^{2n})\sigma$ . When the slot approaches the infinite, i.e.,  $n \to \infty$ , then  $\sigma_0 = \sigma$ . As a consequence, a MS handoff rate H in small cell networks is given by

$$H = \frac{2\sqrt{6}\sigma}{3\sqrt{\pi}r}. (15)$$

Furthermore, the small cell handoff rate is defined as the product of a MS handoff rate and the MS number in a small cell, which is derived by

$$R = H \cdot \lambda_M \cdot \pi r^2 = \frac{2\sqrt{6\pi}\sigma \cdot r \cdot \lambda_M}{3}.$$
 (16)

### III. BACKHAUL TRAFFIC MODELS BASED ON GAUSS-MARKOV MOBILE MODELS

#### A. Backhaul link architecture in small cell networks

A typical backhaul link architecture of small cell networks is illustrated in Fig. 4 (a). In Fig. 4(a), backhaul links are used for connecting two types of cellular scenarios: one type of connection scenario is between the small cell

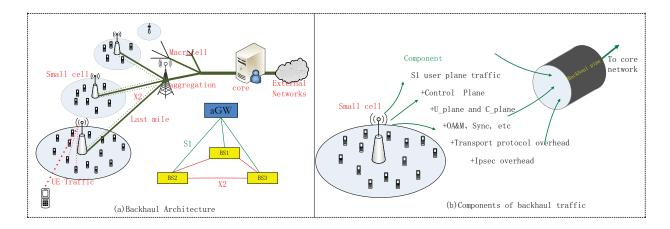


Fig. 4. Backhaul architecture of small cell networks.

and the macro cell, which is connected by S1 links; the other type of connection scenario is among small cells, which is connected by X2 links. Moreover, the logical architecture of backhaul links is illustrated in the lower left corner of Fig. 4(a), where all backhaul links are connected with external networks by the advanced gateway (aGW). Based on the specification in [16], different types of backhaul traffic in small cell networks are explained in Fig. 4(b).

The X2 link can be further classified into two types. One type of X2 link is used for transmitting the handoff management information, which is defined as the X2-C link [20]. For one handoff process in small cells, the management information transmitted by the X2-C link is about 250 bits. Another type of X2 link is used for transmitting the handoff data traffic, which is defined as the X2-U link. For example, one of typical video traffic transmitted by X2-U links is about 353.8 Kbps [21]. Compared with traffic transmitted by X2-U links, the traffic transmitted by X2-C links is ignored in this paper. Therefore, only the traffic transmitted by X2-U links is calculated into X2 links of small cell backhaul networks.

## B. X2 Backhaul Traffic Models

Let  $a_k$  is the offered load for the type-k,  $k \in [1, K]$ , user traffic over X2-U links. Assuming that the type-k user traffic over X2-U links in a small cell follows a Poisson process with an arrive rate  $\omega_k$ . The user session duration, which refers to the time duration of a requested session connection, is assumed to be an exponential distribution with mean  $1/\tau_k$ . Therefore, the active probability of the type-k user traffic is expressed as

$$p_A(k) = \omega_k / (\omega_k + \tau_k). \tag{17}$$

When the handoff duration is denoted as T, the offered load for the type-k user traffic over X2-U links is derived by

$$a_k = p_A(k) RT. (18)$$

The handoff number of the type-k user traffic over X2-U links is denoted as  $\chi_k$ . Furthermore, the handoff number of different K types user traffic over X2-U links is defined by the random vector  $\overrightarrow{\chi} = \{\chi_1, \dots, \chi_k, \dots, \chi_K\}$ . Assuming that all handoff requests over X2-U links are accepted, the stationary distribution of  $\overrightarrow{\chi}$  is derived by

$$P\left(\overrightarrow{\chi}\right) = \prod_{k=1}^{K} \frac{a_k^{\chi_k}}{\chi_k!} e^{-a_k}.$$
 (19)

Moreover, the flow speed of the type-k user traffic over X2-U links is denoted as  $q_k$ . Similarly, the flow speed of different K types user traffic over X2-U links is defined by the random vector  $\overrightarrow{q} = \{q_1, \dots, q_k, \dots, q_K\}$ . Hence, the total traffic caused by handoff in small cells is derived by

$$T_{X2-U} = \sum_{k=1}^{K} \chi_k q_k. \tag{20}$$

Given the bandwidth of X2-U link as  $C_{X2-U}$ , the overflow probability  $P_{OUT}$  is expressed as

$$P_{OUT} = 1 - \sum_{\overrightarrow{\chi}} P(\overrightarrow{\chi}), \quad \Omega = \{ \overrightarrow{\chi} : T_{X2-U} \leqslant C_{X2-U} \}.$$
 (21)

To evaluate the performance of overflow probability in small cell networks, default parameters are configured as [20], [21]: the user density is  $\lambda_M = 0.007 \text{ m}^{-2}$ , the standard deviation of speed is  $\sigma = 1$ , the radius of small cell is r = 50 m. Without loss of generality, there are two types of application traffic. One is voice traffic with transmission speed  $q_1 = 12.2$  Kbps. The other is video traffic with transmission speed  $q_2 = 353.8$  Kbps. The arrive rate of voice and video traffic are configured as  $\omega_1 = 1.5$  and  $\omega_2 = 0.5$ , respectively. The user session duration of voice and video traffic are configured as  $\tau_1^{-1} = 0.033$  and  $\tau_2^{-1} = 0.05$ , respectively. Based on the exhaustion approach over the set  $\Omega$ , the overflow probability is simulated in Fig. 5. When the radius of small cells is fixed, the overflow probability decreases with the increase of the X2-U bandwidth. When the X2-U bandwidth is fixed, the overflow probability increases with the increase of the radius of small cells.

#### C. S1 backhaul traffic models

S1 links are used for exchanging user data traffic between small cells and the external networks. Many empirical measurement results have demonstrated that the traffic load in both wired and wireless networks, including cellular networks, is self-similar and bursty [22], [23]. Self-similar traffic models, e.g., Pareto distributions with the infinite variance, have gained significant attention in traffic modeling of wireless networks [24]. To evaluate the impact of self-similar traffic load on S1 links, the spatial traffic intensity  $\beta(x_{MS})$  at a MS is assumed to be governed by a Pareto distribution with the infinite variance in this paper. Moreover, the spatial traffic intensity of all MSs is assumed to be independently and identically distributed (i.i.d.). Then, a PDF of spatial traffic intensity is given by

$$f_{\beta}(x) = \frac{\theta \beta_{\min}^{\theta}}{x^{\theta+1}}, \ x \geqslant \beta_{\min} > 0, \tag{22}$$

where  $\theta \in (1,2]$  reflects the heaviness of the distribution tail. When the value of heaviness index  $\theta$  is closer to one, the distribution tail of spatial traffic intensity becomes heavier. This result implies slower decaying in the tail of PDF curve and more burstiness in the defined traffic load. Parameter  $\beta_{\min}$  represents the minimum traffic rate

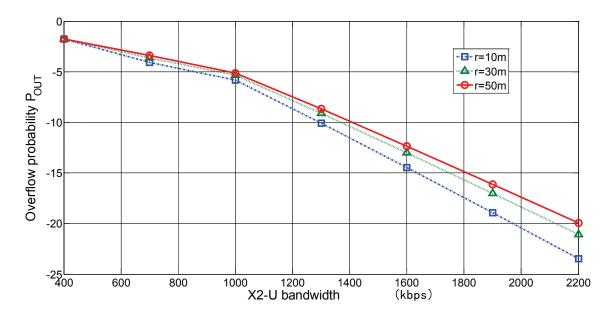


Fig. 5. Overflow probability with respect to the X2-U bandwidth considering different radii of small cells.

preserved for MS's quality of service (QoS) guarantee. Furthermore, the average spatial traffic intensity of MSs is expressed by

$$\mathbb{E}\{\beta\} = \int_{\Omega} \varphi \cdot f_{\beta}(\varphi) \, d\varphi = \frac{\theta \beta_{\min}}{\theta - 1},\tag{23}$$

where the integral range of  $\varphi f_{\beta}(\varphi)$  is  $(\beta_{\min}, +\infty)$ . As a consequence, the average S1 traffic model in a small cell is derived by

$$T_{S1} = \lambda_M \cdot A_{C0} \cdot \mathbb{E}\{\beta\}$$

$$= \lambda_M \cdot \pi r^2 \cdot \frac{\theta \beta_{\min}}{\theta - 1},$$
(24)

where  $A_{C0}$  is the coverage area of small cell. Considering the regular hexagon structure of small cells, the coverage area of small cell is approximated by  $A_{C0} = \pi \cdot r^2$ .

To analysis the average S1 traffic in a small cell, some default parameters are configured as [25]: the heaviness index is  $\theta = 1.8$  and the minimum traffic rate is  $\beta_{\min} = 10.75$ . Fig. 6 illustrates the impact of the radius of small cell and the MS density on the average S1 traffic in a small cell. When the MS density is fixed, the average S1 traffic increases with the increase of the radius of small cell. When the radius of small cell is fixed, the average S1 traffic increases with the increase of the MS density in a small cell.

To evaluate the relationship between the X2-U traffic and the S1 traffic, the ratio of the X2-U traffic to the S1 traffic is defined as

$$\phi = \frac{T_{X2-U}}{T_{S1}}. (25)$$

Furthermore, the impact of the radius of small cell and the speed standard deviation on the ratio of X2-U traffic to the S1 traffic is analyzed in Fig. 7. Without loss generality, the overflow probability is configured as  $P_{OUT} = 10^{-4}$ 

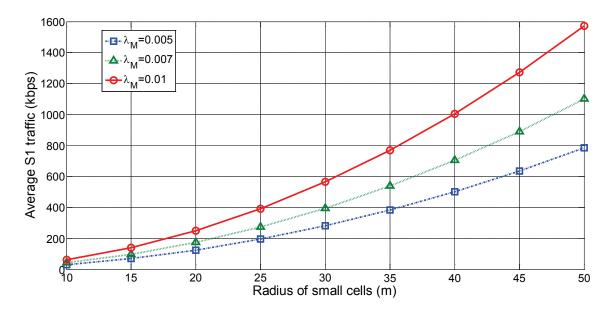


Fig. 6. Average S1 traffic with respect to the radius of small cell and the MS density in a small cell.

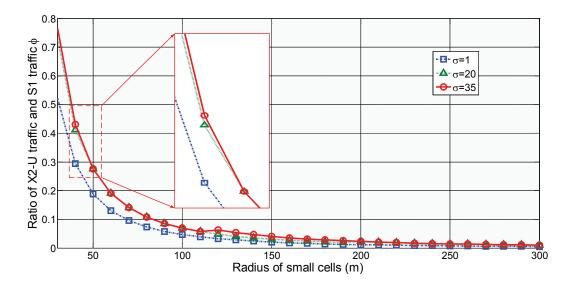


Fig. 7. Ratio of X2-U traffic to the S1 traffic with respect to the radius of small cell and the speed standard deviation.

in Fig. 7. When the radius of small cell is fixed, the ratio of X2-U traffic to the S1 traffic increases with the increase of the speed standard deviation. When the speed standard deviation is fixed, the ratio of X2-U traffic to the S1 traffic decreases with the increase of the radius of small cell. When the radius of small cell is less than 50 m, the ratio of X2-U traffic to the S1 traffic is larger than 20%. This result implies that the X2-U traffic used for handoff is obviously increased. When the radius of small cell is larger than 200 m, the ratio of X2-U traffic to the S1 traffic is approach 4%. These results are validated by the real measurement results in [21] and [26].

#### IV. ENERGY EFFICIENCY OF SMALL CELL BACKHAUL NETWORKS

### A. Energy efficiency models of small cell backhaul networks

Based on the logical architecture of small cell networks in Fig. 4, backhaul traffic links include X2 links and S1 links which are used for transmitting handoff information and user data traffic, respectively. For a small cell, the uplink backhaul traffic only includes the X2 link traffic, which is given as

$$TH_{small-up} = T_{X2-U}. (26)$$

For a small cell, the downlink backhaul traffic includes the X2 links traffic and the S1 links traffic, which is given as

$$TH_{small-down} = T_{S1}^{small} + T_{X2-U}. (27)$$

Similarly, the uplink backhaul traffic of macrocell includes the X2 link traffic and the downlink backhaul traffic of macrocell includes the X2 link traffic and the S1 link traffic. However, the density of macrocells is obviously less than the density of small cells. The X2 link traffic of macrocell is also obviously less than the X2 link traffic of small cells. Therefore, the X2 link traffic is ignored for the macrocell backhaul traffic in this paper. As a consequence, the downlink backhaul traffic of macrocell is given by

$$TH_{macro-down} \approx T_{S1}^{macro}$$
. (28)

Assuming that M small cells are scattered into a macrocell, all of M small cells and a macrocell are formed a small cell network in this paper. Therefore, the total backhaul traffic of a small cell network is given by

$$TH_{sum} = TH_{sum-up} + TH_{sum-down}, (29a)$$

$$TH_{sum-up} = M \cdot TH_{small-up} + TH_{macro-up}, \tag{29b}$$

$$TH_{sum-down} = M \cdot TH_{small-down} + TH_{macro-down}.$$
 (29c)

A BS energy consumption can be decomposed into the embodied energy consumption part and the operating energy consumption part [11]. The embodied energy consumption  $E_{EM}$  is the energy consumed by all processes associated with the production of a BS. The operating energy consumption  $E_{OP}$  is the energy consumed for the BS operation in the lifetime. The operating energy is further divided into two parts: the dynamical part  $E_{OPlin}$ , which is linearly scaled with the transmission power, representing the power amplifier and feeder losses, cooling, etc.; the constant part  $E_{OPconst}$ , representing by the fixed energy consumed by signal processing, battery backup, etc. Hence, the BS operating energy is given by

$$E_{\rm OP} = E_{\rm OPlin} + E_{\rm OPconst}.$$
 (30)

Moreover, the linear relation of BS's operating power  $P_{OP}$  to its transmission power  $P_{TX}$  is expressed as

$$P_{\text{OP}} = e \cdot P_{\text{TX}} + d, \ e > 0 \text{ and } d > 0.$$
 (31)

In general, the transmission power depends on the radius of cell coverage and the signal propagation fading. To simplify the derivation, the macrocell BS transmission power is normalized as  $P_0 = 40$  Watt (W) with the cell

Cell type	Macrocell(5.8 GHz)	Small Cell(60 GHz)		
	(r=500 m)	(r=20 m)	(r=30 m)	(r=50 m)
e	21.45	7.84	7.84	7.84
d	354.44 W	71.50 W	71.50 W	71.50 W
$P_{TX}$	4.35 W	57.3 mW	293.86 mW	1322.31 mW
$P_{OP}$	447.80 W	71.95 W	73.80 W	81.87 W
Embodied energy	85 GJ	20% of total energy		
Lifetime	10 years	5 years		

TABLE I
PARAMETERS FOR NUMERICAL SIMULATIONS.

radius  $r_0 = 1$  Kilometer (Km) [7]. Considering the path loss in the signal propagation fading, the BS transmission power with the cell radius r is expressed as

$$P_{TX} = P_0 \cdot (r/r_0)^{\gamma},\tag{32}$$

where  $\gamma$  is the path loss coefficient. The BS operating power is derived by

$$P_{\text{OP}} = e \cdot P_0 \cdot (r/r_0)^{\gamma} + d. \tag{33}$$

As a consequent, in the whole lifetime  $T_{lifetime}$ , the BS dynamical operating energy is given by

$$E_{\text{OPlin}} = P_{\text{OP}} \cdot T_{lifetime}. \tag{34}$$

When M small cells are overlapped with the macrocell, the system energy consumption of M small cells and a macrocell is expressed as

$$E_{system} = E_{EM}^{macro} + E_{OP}^{macro} + M \cdot \left( E_{EM}^{small} + E_{OP}^{small} \right)$$

$$= E_{EM}^{macro} + P_{OP}^{macro} \cdot T_{lifetime}^{macro} + M \cdot \left( E_{EM}^{small} + P_{OP}^{small} \cdot T_{lifetime}^{small} \right),$$
(35)

where  $E_{EM}^{macro}$ ,  $P_{OP}^{macro}$  and  $T_{lifetime}^{macro}$  are the embodied energy, the operating energy and the lifetime of macrocell BS, respectively;  $E_{EM}^{small}$ ,  $P_{OP}^{small}$  and  $T_{lifetime}^{small}$  are the embodied energy, the operating energy and the lifetime of small cell BS, respectively. Furthermore, the energy efficiency of small cell networks is derived by

$$\eta_{EE} = \frac{TH_{sum}}{E_{system}}$$

$$= \frac{M \cdot (T_{S1}^{small} + 2T_{X2-U}) + T_{S1}^{macro}}{E_{EM}^{macro} + E_{OP}^{macro} + M \cdot (E_{EM}^{small} + E_{OP}^{small})}.$$
(36)

## B. Performance analysis and discussion

To evaluate the energy efficiency of small cell networks, some default parameters are configured as follows [11], [27], [28]: the radius of macrocell is 500 m; the radius of small cell is 50 m; the frequency of macrocell BS is 5.8 GHz and the frequency of small cell BS is 60 GHz, i.e., millimeter frequency band; parameters of macrocell BS operating power are configured as e = 21.45 and d = 354.44 W, respectively; parameters of small cell BS operating

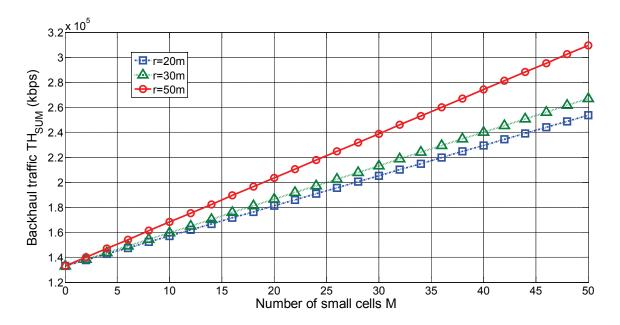


Fig. 8. Total backhaul traffic of small cell network with respect to the number and radius of small cell.

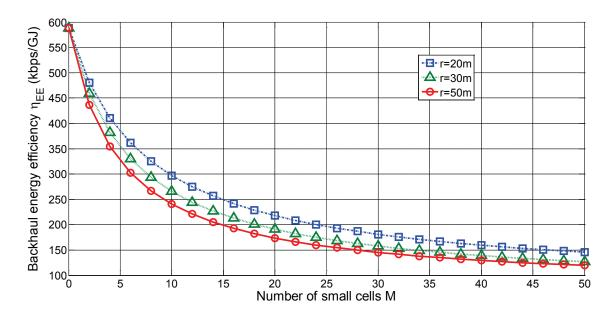


Fig. 9. Energy efficiency of small cell backhaul network with respect to the number and radius of small cells.

power are configured as e = 7.84 and d = 71.50 W; the path loss coefficient is 3.2 for urban environments. More detail simulation parameters are list in Table 1.

Fig. 8 shows the total backhaul traffic of small cell network with respect to the number and radius of small cells. When the radius of small cell is fixed, the total backhaul traffic linearly increases with the increase of the number

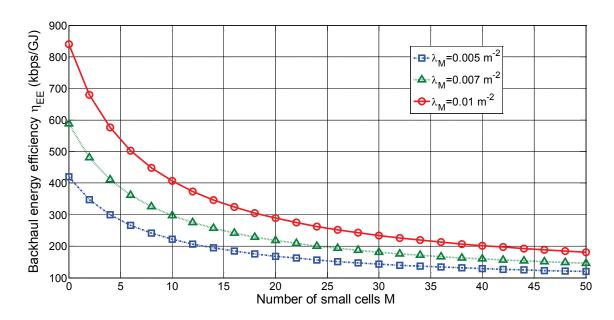


Fig. 10. Energy efficiency of small cell backhaul network with respect to the number of small cells and the MS density in a small cell.

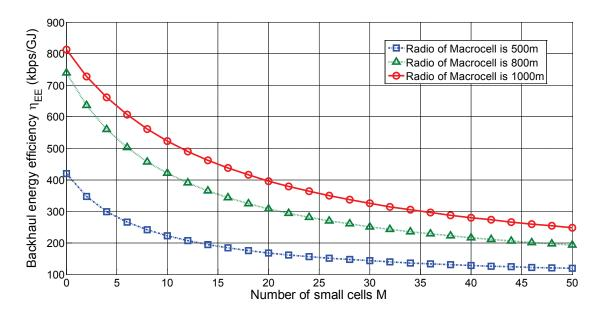


Fig. 11. Energy efficiency of small cell backhaul network with respect to the number of small cells and the radius of macrocell.

of mall cells. When the number of small cells is fixed, the total backhaul traffic increases with the increase of the radius of small cells.

Fig. 9 illustrates the energy efficiency of small cell backhaul network with respect to the number and radius of small cells. When the radius of small cell is fixed, the energy efficiency exponentially decreases with the increase of the number of small cells. When the number of small cells is fixed, the energy efficiency decreases with the

increase of the radius of small cells.

In Fig. 10, the energy efficiency of small cell backhaul network is depicted with different MS densities in a small cell. When the number of small cells is fixed, the energy efficiency of small cell backhaul network increases with the increase of the MS density in a small cell. Finally, Fig. 11 evaluates the energy efficiency of small cell backhaul networks with different radius of macrocells. When the number of small cells is fixed, the energy efficiency of small cell backhaul network increase with the increase of the radius of macrocells.

#### V. CONCLUSION

In this paper, an energy efficiency of small cell backhaul networks using Gauss-Markov mobile models is proposed. Based on the Gauss-Markov mobile models, a handoff rate of small cell networks is presented. Furthermore, backhaul traffic models of X2 and S1 links are proposed for small cell networks. The energy efficiency model considering the embodied energy and operating energy is proposed for the small cell backhaul network. Numerical results imply that the energy efficiency of small cell backhaul network decreases with the number of small cells and increases with the density and coverage of macrocells. These results provide some useful guidelines to deploy the number of small cells in small cell networks. For the future work, we plan to investigate the energy efficiency of small cell backhaul networks with stochastic geometry coverage scenarios.

#### REFERENCES

- [1] Li C. and Chao H.: 'IPv6 auto-configuration VANET Cross Layer Design Based on IEEE 1609', IET Networks, December 2012, 1, (4), pp. 199-206
- [2] Hu C., Lai C., Huang Y. and Chao H.: 'A Two-Tier Framework for Transmission-Cost Minimization of High Performance Communication Applications', Concurrency and Computation: Practice and Experience, March 2012, 24, (4), pp.383-395
- [3] Hoydis, J., Kobayashi, M., Debbah, M.: 'Green small-cell networks', IEEE Vehicular Technology Magazine, 2011, 6, (1), pp. 37-43
- [4] Ji, B., Lu, Z., Song, K., et al.: 'The performance analysis and access mechanism of small cell network', Vehicular Technology Conference (VTC Fall), Las Vegas, USA, September 2013, pp. 1-6
- [5] Guruacharya, S., Niyato, D., Bennis, M., et al.: 'Dynamic coalition for network MIMO in small cell networks', IEEE Transactions on Wireless Communications, 2013, 12, (10), pp. 5360 5372
- [6] Gharbi, N., Mokdad, L., Ben-Othman, J.: 'Performance and reliability analysis of Small Cell Networks with retrials and different breakdowns disciplines: A computational approach', Computers and Communications (ISCC), Split, Croatia, July 2013, pp. 85-90
- [7] Yamamoto, T., Konishi, S.: 'Impact of small cell deployments on mobility performance in LTE-Advanced systems', Personal, Indoor and Mobile Radio Communications (PIMRC Workshops), 2013 IEEE 24th International Symposium on, London, UN, September 2013, pp. 189-193
- [8] Chen, C.S., Nguyen, V.M., Thomas, L.: 'On small cell network deployment: a comparative study of random and grid topologies', Vehicular Technology Conference (VTC Fall), Quebec City, Canada, September 2012, pp. 1-5
- [9] Chang J., Lai C., Chao H., Zhu R.: 'An Energy-efficient Geographic Routing Protocol Design in Vehicular Ad-hoc Network', Computing, February 2014, pp. 119-131.
- [10] Hasan, Z., Boostanimehr, H., Bhargava, V.K.: 'Green cellular networks: a survey, some research issues and challenges', IEEE Communication Surveys and Tutorials, 2011, 13, (4), pp. 524-540
- [11] Humar, I., Ge, X., Xiang, L., et al.: 'Rethinking energy efficiency models of cellular networks with embodied energy', IEEE Network, 2011, 25, (2), pp. 40-49
- [12] Li, C., Zhang, J., Letaief, K.B.: 'Energy efficiency analysis of Small Cell networks', Communications (ICC), 2013 IEEE International Conference on, Budapest, Hungary, June 2013, pp. 4404 4408
- [13] Ge, X., Han, T., Zhang, Y., et al.: 'Spectrum and Energy Efficiency Evaluation of Two-Tier Femtocell Networks with Partially Open Channels', IEEE Transactions on Vehicular Technology, 2014, 63, (3), pp. 1306 1319
- [14] Li, C., Zhang, J., Letaief, K.B.: 'Throughput and energy efficiency analysis of small cell networks with multi-antenna base stations', IEEE Transactions on Wireless Communications, 2014, 13, (5), pp. 2505 2517
- [15] Wang, W., Shen, G.,: 'Energy efficiency of heterogeneous cellular network', Vehicular Technology Conference Fall (VTC 2010-Fall), 2010 IEEE 72nd, Ottawa, Canada, September 2010, pp. 1-5

- [16] Robson, J.: 'Small cell backhaul requirements', NGMN White Paper, June 2012, pp.1-40
- [17] Jungnickel, V., Manolakis, K., Jaeckel, S., et al.: 'Backhaul requirements for inter-site cooperation in heterogeneous LTE-Advanced networks', Communications Workshops (ICC), 2013 IEEE International Conference on, Budapest, Hungary, June 2013, pp. 905-910
- [18] Samardzija, D., Huang, H.: 'Determining backhaul bandwidth requirements for network MIMO', 17th European Signal Processing Conference (EUSIPCO), Glasgow, Scotland, August 2009, pp. 1494-1498
- [19] Robson, J.: 'Guidelines for LTE backhaul traffic estimation', NGMN White Paper, July 2011, pp. 1-18
- [20] 3GPP TS 36.423: 'X2 Application Protocol (X2AP)', http://www.3gpp.org/ftp/specs/archive/36\_series/636.423/, accessed June 2008
- [21] Widjaja, I., La Roche, H.: 'Sizing X2 Bandwidth For Inter-Connected eNodeBs', Vehicular Technology Conference Fall (VTC 2009-Fall), 2009 IEEE 70th, Anchorage, USA, September 2009, pp. 1-5
- [22] Ge X., Yang Y., Wang C.-X., Liu Y.: 'Characteristics Analysis and Modeling of Frame Traffic in 802.11 Wireless Networks', Wireless Communications and Mobile Computing (Wiley InterScience), 2010, 10, (4), pp.584-592
- [23] Paxson, V., Floyd, S.: 'Wide-area traffic: the failure of poisson modeling', IEEE/ACM Transactions on Networking, 1995, 3, (3), pp. 226-244
- [24] Xiang, L., Ge, X., Wang, C.-X., et al.: 'Energy efficiency evaluation of cellular networks based on spatial distributions of traffic load and power consumption', IEEE Transactions on Wireless Communications, 2013, 12, (3), pp.961-973
- [25] 3GPP. TS 25.101: 'User Equipment (UE) radio transmission and reception (FDD)', http://www.3gpp.org/ftp/specs/archive/25\_series/25.101/, accessed June 2011
- [26] Huawei: 'LTE requirements for bearer networks', Huawei Publications, http://www.huawei.com/publications/view.do?id=5904&cid=10864&pid=61/, accessed June 2009
- [27] Richter, F., Fehske, A.J., Fettweis, G.P.: 'Energy efficiency aspects of base station deployment strategies for cellular networks', Vehicular Technology Conference Fall (VTC 2009-Fall), 2009 IEEE 70th, Anchorage, USA, September 2009, pp. 1-5
- [28] Khirallah, C., Thompson, J.S., Rashvand, H.: 'Energy and cost impacts of relay and femtocell deployments in long-term-evolution advanced', IET communications, 2011, 5, (18), pp. 2617-2628